

Settlement analysis of isolated footings using two soil models

Stefan Mihajlović^{1*}, Iva Despotović¹, Jovana Bojković¹,
Marijana Janičijević Milačak¹, Vladimir Mandić¹

¹ University of Kragujevac, Faculty of Mechanical and Civil engineering in Kraljevo, Serbia

ARTICLE INFO

* **Correspondence:** mihajlovic.s@fmgkv.kg.ac.rs

DOI: 10.5937/engtoday2600006M

UDC: 621(497.11)

ISSN: 2812 – 9474

Article history: Received 28 January 2026; Revised 27 February 2026; Accepted 28 February 2026

ABSTRACT

This paper investigates the influence of soil idealization on stress distribution and settlement beneath isolated footings of building structures. Two basic soil models commonly used in geotechnical engineering practice are analyzed: the elastic half-space model and the finite-thickness soil layer model resting on a rigid base. Stress and settlement analyses were performed for square isolated footings of different dimensions subjected to a constant uniformly distributed surface load, while varying the mechanical properties of the soil. Particular attention is devoted to comparing the soil deformation response at characteristic points along the footing–soil interface. The obtained results indicate a significant influence of the selected soil model, soil deformability (soil stiffness, E), and footing geometry on settlement values, confirming the necessity of a careful choice of the calculation model in geotechnical design.

KEYWORDS

Geotechnical modeling, Elastic half-space soil model, Finite soil layer model, Shallow foundations, Isolated footing.

1. INTRODUCTION

Soil modeling beneath building structures represents one of the key aspects of geotechnical and structural design, as it directly affects stress distribution at the footing–soil interface as well as the magnitude and character of soil settlements. The stresses transferred from the structure to the soil depend on the stiffness of the footing, the mechanical properties of the soil, and the geometry of the contact surface; inaccurate assessment may lead to exceeding allowable soil stresses [1]. The consequences of such conditions include uneven settlements, cracking of structural elements, and a reduction in structural bearing capacity. Therefore, a realistic numerical or analytical model of soil–foundation interaction is essential for a reliable assessment of structural behavior during service life [2]. This issue is particularly significant for isolated footings, which—unlike strip footings and raft foundations—behave as independent structural systems. Due to the relatively small area through which the load is transferred to the soil, isolated footings induce higher stress concentrations and more pronounced local settlements [3]. These settlements may be differential relative to adjacent foundations, leading to additional internal forces in the superstructure. Consequently, accurate soil modeling beneath isolated footings is crucial to ensure the safety, serviceability, and durability of the entire structure [4]. In the early stages of geotechnical engineering development, soil models were based on simplified assumptions in which the soil beneath structures was treated as a homogeneous and isotropic medium. Such models assumed exclusively elastic deformations that were linearly related to applied stress. One of the most well-known examples of this approach is the Winkler soil model, in which the soil is idealized as a system of independent springs [2]. This model is directly based on Hooke's law and enables a simplified analysis of soil–

foundation interaction. However, practical experience and experimental investigations have shown that soil behavior cannot be fully described using purely elastic laws. Under structural loading, both elastic and plastic deformations occur in the soil, with plastic deformations potentially being permanent and significantly affecting foundation settlement [5]. As a result, more advanced constitutive soil models have been developed to realistically describe nonlinear behavior and stress-history dependency [6]. These models allow for more accurate determination of stresses at the footing–soil interface as well as total and differential settlements. Modern soil modeling approaches based on the finite element method include various constitutive soil models, such as the linear elastic model [7], the elasto-plastic Mohr–Coulomb model [8], the Hardening Soil model [9], the Modified Cam-Clay model [10], and advanced hypoplastic models [11]. Their primary advantage lies in the ability to represent layered soil profiles, nonlinear behavior, plastic deformation, and soil–structure interaction under complex loading conditions. This enables detailed stress distribution analysis and reliable prediction of total and differential settlements. However, the main disadvantages include strong dependence of results on the selected constitutive model and input parameters, increased data requirements, and higher computational complexity compared to simpler analytical approaches [12].

In soil–foundation interaction analyses, two basic idealized soil models are most commonly considered [3]. The first is the elastic half-space model, in which the soil is treated as a continuum extending infinitely in depth [13]. It is referred to as a half-space because it is bounded at the top by the plane representing the contact surface between the foundation and the soil. This idealization is particularly suitable for stress and settlement analyses when deep soil layers are significantly thicker than the foundation dimensions [14]. The second approach considers soil as a finite-thickness layer, accounting for the presence of a rigid or significantly stiffer layer at a certain depth [15]. In this case, stress distribution and settlement magnitude depend not only on soil properties but also on the depth and characteristics of the lower boundary. This model is more realistic for sites where bedrock or very dense soil exists beneath the bearing layer and enables a more accurate assessment of settlements under conditions of limited soil deformability. The present study analyzes stress and settlement results beneath an isolated footing using both soil modeling approaches: the elastic half-space model and the finite-thickness soil layer model. The main objective of the paper is to highlight differences in results obtained using these models and to provide practical recommendations for their application in engineering practice.

2. METHODS

In the numerical analyses, the soil beneath the foundation is modeled as a continuum using three-dimensional finite elements with appropriate material properties. Theoretically, the elastic half-space is bounded at the top by the ground surface and extends infinitely in depth and width. The soil is characterized by its deformation modulus, also referred to as soil stiffness (E), Poisson's ratio, and unit weight. Due to the complexity of this modeling approach, it is necessary to reasonably estimate the dimensions of the analyzed domain, thereby simplifying the numerical model while maintaining acceptable accuracy.

2.1. Soil Modeled as an Elastic Half-Space of Infinite Thickness

In this study, the soil beneath the isolated footing is modeled as an elastic half-space of infinite thickness, bounded at the top by the footing–soil contact plane [16]. The soil is assumed to be homogeneous, isotropic, and continuous, behaving according to the laws of linear elasticity. The load is transferred from the footing to the soil through a finite contact area, and the distribution of normal stresses and the soil deformation response are analyzed. This approach allows analytical or semi-analytical determination of the stress state and settlement beneath the isolated footing. Figure 1 shows a rigid footing resting on a single-layer soil represented as an elastic continuum. Soil properties are described by Poisson's ratio μ and the soil deformation modulus (soil stiffness) E .

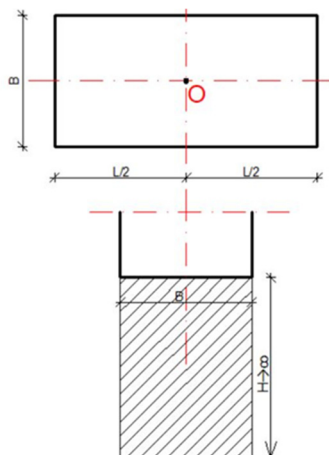


Figure 1: Soil model as an elastic half-space of infinite thickness beneath an isolated footing

The problem of determining stresses and displacements induced by a uniformly distributed vertical load over a rectangular area was studied by Newmark, Steinbrenner, and Florin. Vertical stresses along the axis passing through the center point (O) are expressed using established analytical solutions. Corresponding expressions allow calculation of vertical displacements, i.e., settlements, as functions of load intensity, footing geometry, soil stiffness (E), and Poisson's ratio:

$$\sigma_z = \frac{2p}{\pi} \left(\operatorname{arctg} \frac{ab}{z\sqrt{a^2 + b^2 + z^2}} + \frac{abz(a^2 + b^2 + 2z^2)}{(a^2 + z^2)(b^2 + z^2)\sqrt{a^2 + b^2 + z^2}} \right) \quad (1)$$

where:

p – intensity of the applied uniformly distributed vertical load, z – coordinate along the z -axis, i.e., the depth within the elastic half-space, and a and b – coordinates in the horizontal plane defining the position of the axis along which the vertical stresses are evaluated.

By substituting the known geometric parameters and the physical–mechanical properties of the materials involved in the soil–foundation interaction into the above expression, the calculation of vertical stresses is reduced to the following form:

$$\sigma_z = p I_{43} \quad (2)$$

where:

p – intensity of the applied uniformly distributed vertical load, I_{43} – tabulated coefficient depending on the soil type (defined by Poisson's ratio μ) and the geometric characteristics of the footing (expressed by the length-to-width ratio L/B) [3]. The displacement components in the direction of the z -axis can be determined using the following expression:

$$w = \frac{P(1+\mu)}{2\pi E} \frac{1}{R} \left(\frac{z^2}{R^2} + 2(1-\mu) \right) \quad (3)$$

The values of the elastic constants of the medium, m and G , are given by expressions that depend on the soil deformation modulus (soil stiffness) E and Poisson's ratio μ :

$$m = \frac{1}{\mu}; \quad G = \frac{E}{2(1+\mu)} \quad (4)$$

By substituting the known geometric parameters and the physical–mechanical properties of the materials involved into the preceding settlement expression, the calculation of deformations (settlements) is reduced to the following form:

$$w = \frac{pB}{E} I_{53} \quad (5)$$

where:

p – intensity of the applied uniformly distributed vertical load, B – width of the considered footing, E – soil deformation modulus (soil stiffness), and I_{53} – tabulated coefficient depending on the soil type (defined by Poisson's ratio μ) and the geometric characteristics of the footing (expressed by the length-to-width ratio L/B).

The main advantage of the infinite half-space model lies in its mathematical simplicity and clearly defined assumptions, enabling relatively fast and stable estimation of stresses and settlements. The model is particularly suitable for isolated footings, where loads are transferred through a relatively small area and the influence of deep soil layers is dominant. However, its main limitation is the neglect of soil layering and the presence of a rigid base at finite depth, which may lead to deviations from real soil behavior. Additionally, the assumption of purely elastic behavior does not account for plastic deformations, potentially leading to underestimated settlement values under higher loads.

2.2. Soil Modeled as a Finite-Thickness Layer

Soil–foundation interaction can also be analyzed for cases in which the soil layer beneath the footing–soil interface has a finite thickness. In this approach, the stress and deformation calculation procedure is similar to that of the half-space model, but boundary conditions differ. Soil properties are again defined by Poisson's ratio μ and soil stiffness E . In comparison with the infinite half-space model, stress and deformation distributions additionally depend on the thickness of the compressible soil layer. This modeling approach is commonly applied when soil layer thicknesses and

their mechanical properties are known to a certain depth, below which a rigid or incompressible layer exists. Figure 2 illustrates the geometry and boundary conditions of this soil model.

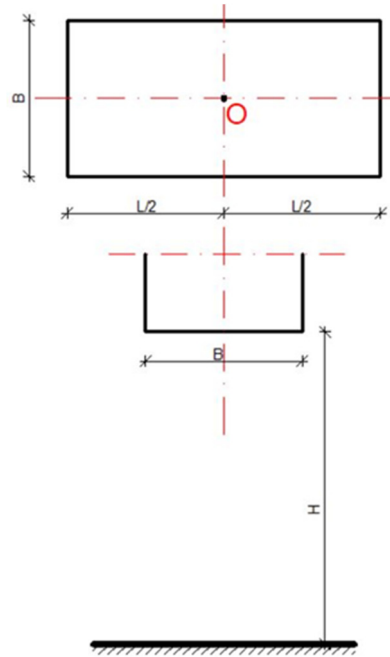


Figure 2: Soil model as a finite-thickness layer beneath an isolated footing

The problem of determining stresses and deformations (settlements, w) induced by a uniformly distributed load acting through a flexible rectangular footing has been investigated by several researchers. For the purpose of determining stress components and displacements in the soil caused by a uniformly distributed vertical load, the following assumptions are adopted: the footing is flexible and rectangular in shape; the compressible soil layer is elastic and isotropic; its thickness is limited by an incompressible base; and the contact between the footing and the soil is assumed to be smooth in one case and fully rough in the other. The vertical stresses, σ_z , are given by the following expression:

$$\sigma_z = \sum_m \sum_n \left(\alpha A_{12} U + \beta A_{12} V + A_{11} \frac{dW}{dz} \right) \cos \alpha x \cos \beta y \tag{6}$$

The integration constants in the above expression are determined from the boundary conditions. The displacements w for the case of smooth contact is given by the following expression:

$$w_{m,n} = \frac{1}{2G} \left\{ \left[(3 - 4\mu) C_4 - C_2 \gamma \right] \text{sh } \gamma z - C_4 \gamma z \text{ch } \gamma z \right\} \tag{7}$$

The displacements w for the case of rough contact is given by the following expression:

$$w_{m,n} = \frac{1}{2G} \left\{ \left[(3 - 4\mu) C_4 - \gamma z C_3 \right] \text{sh } \gamma z - \gamma z C_4 \text{ch } \gamma z \right\} \tag{8}$$

where:

C_2, C_3 , and C_4 – integration constants given in [18], and G – value of the elastic constant of the medium. By substituting the known geometric parameters and the physical–mechanical properties of the materials into the above expression, the calculation of vertical stresses is reduced to the following form:

$$\sigma_z = p I_{109} \tag{9}$$

where:

p – intensity of the applied uniformly distributed vertical load, I_{109} – tabulated coefficient depending on the soil type (defined by Poisson’s ratio μ), the geometric characteristics of the footing (expressed by the length-to-width ratio L/B and the ratio of footing width to the depth of the compressible soil layer H/B), and the position of the z -axis along which the vertical stresses are evaluated.

As in the previous model, displacement components can also be calculated for the soil modeled as a finite-thickness layer, for given geometric characteristics and material properties involved in the soil–foundation interaction, using the following expression:

$$w = \frac{p B}{E} I_{112} \tag{10}$$

where:

p – intensity of the applied uniformly distributed vertical load, B – width of the considered footing, E – soil deformation modulus (soil stiffness), and I_{112} – tabulated coefficient depending on the soil type (defined by Poisson’s ratio μ), the geometric characteristics of the footing (expressed by the length-to-width ratio L/B and the ratio of footing width to the depth of the compressible soil layer H/B), and the position of the z -axis depending on the location of the point on the footing–soil contact surface at which the deformations (settlements) are evaluated.

The main advantage of this model lies in its more realistic representation of actual geotechnical conditions, especially when bedrock or very dense soil exists beneath the foundation. This approach generally results in smaller settlement values compared to the infinite half-space model due to constrained soil deformation. However, its disadvantages include increased computational complexity and the requirement for reliable data on soil layer thickness and lower boundary properties.

3. RESULTS AND DISCUSSION

This section presents the results of stress and settlement analyses at the footing–soil interface for the previously described soil models. The analyses were conducted for an isolated footing with a thickness of 0.40 m and square plan dimensions of 2.50 m, 3.25 m, and 4.00 m. A constant uniformly distributed surface load of 200 kPa was applied over the entire contact area.

Soil parameters were defined assuming a Poisson’s ratio of $\nu = 0.30$, while soil deformability (soil stiffness) E was varied between 10 and 50 MPa to cover a wide range of realistic geotechnical conditions. For the finite-thickness soil layer model, a compressible layer thickness of $H = 10$ m was assumed, underlain by a rigid base.

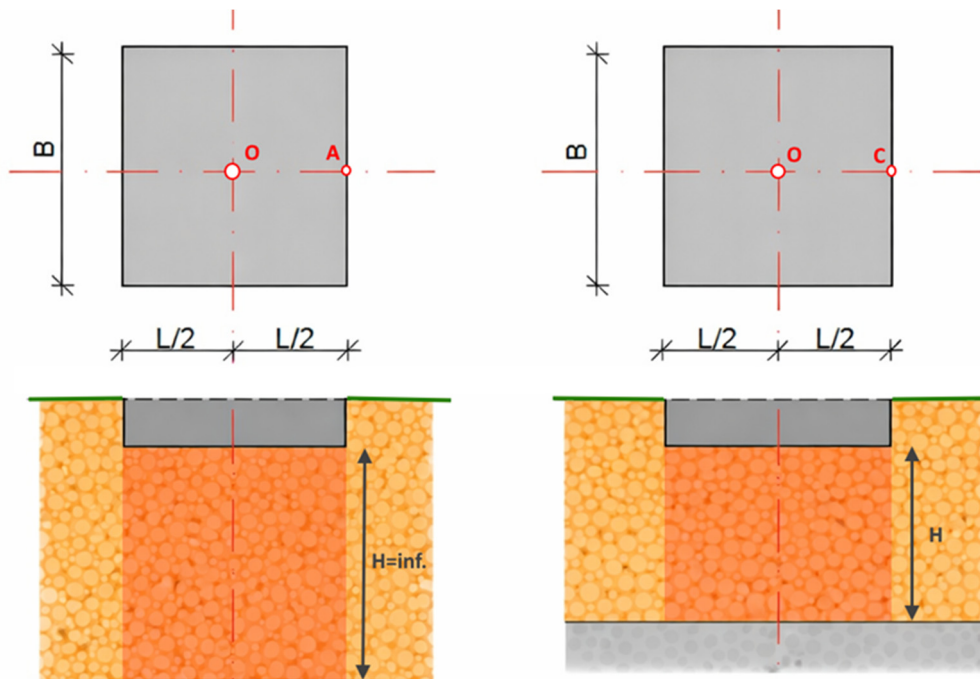


Figure 3: Geometric characteristics of the isolated footing for the two analyzed soil models with control points

The obtained results enable an analysis of the influence of soil stiffness and finite bearing layer thickness on stresses at the footing–soil contact interface and on settlements beneath the isolated footing. The settlement calculation results for the isolated footing obtained using the elastic half-space model and the finite-thickness soil layer model are presented in the following tables.

Table 1: Settlement results for soil modeled as an elastic half-space

E [MPa]	L/B=2.50/2.50m		L/B=3.25/3.25m		L/B=4.0/4.0m	
	w_o [cm]	w_a [cm]	w_o [cm]	w_a [cm]	w_o [cm]	w_a [cm]
10	4.858	3.237	6.316	4.209	7.773	5.180

E [MPa]	L/B=2.50/2.50m		L/B=3.25/3.25m		L/B=4.0/4.0m	
	w _o [cm]	w _a [cm]	w _o [cm]	w _a [cm]	w _o [cm]	w _a [cm]
15	3.239	2.158	4.211	2.806	5.182	3.453
20	2.429	1.619	3.158	2.105	3.860	2.590
25	1.944	1.295	2.527	1.684	3.109	2.072
30	1.620	1.079	2.106	1.403	2.591	1.727
35	1.388	0.925	1.805	1.203	2.221	1.480
40	1.215	0.810	1.579	1.053	1.943	1.295
45	1.080	0.720	1.404	0.936	1.727	1.151
50	0.972	0.648	1.264	0.842	1.555	1.036

Table 2: Settlement results for soil modeled as a finite-thickness layer (H = 10 m)

E [MPa]	L/B=2.50/2.50m		L/B=3.25/3.25m		L/B=4.0/4.0m	
	w _o [cm]	w _c [cm]	w _o [cm]	w _c [cm]	w _o [cm]	w _c [cm]
10	4.498	2.040	5.694	2.502	6.744	2.820
15	2.998	1.360	3.796	1.668	4.496	1.880
20	2.249	1.020	2.847	1.251	3.372	1.410
25	1.799	0.816	2.278	1.001	2.698	1.128
30	1.499	0.680	1.898	0.834	2.248	0.940
35	1.285	0.583	1.627	0.715	1.927	0.806
40	1.124	0.510	1.423	0.626	1.686	0.705
45	0.999	0.453	1.265	0.556	1.499	0.627
50	0.900	0.408	1.139	0.500	1.349	0.564

In the following section, a comparative presentation of the deformation, i.e., soil settlement calculation results obtained using the two analyzed soil models is provided. The subsequent figures illustrate a comparison of soil behavior modeled as an elastic half-space of infinite thickness and as a finite-thickness soil layer. This comparative analysis enables evaluation of the influence of soil idealization on the magnitude and distribution of settlements beneath the isolated footing.

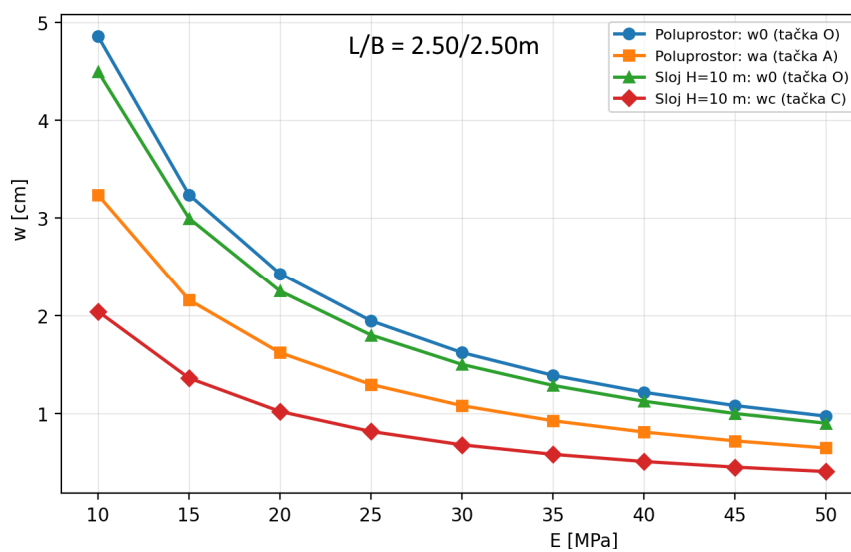


Figure 4: Comparative settlement values for an isolated footing with L/B = 2.50/2.50 m for the two analyzed soil models

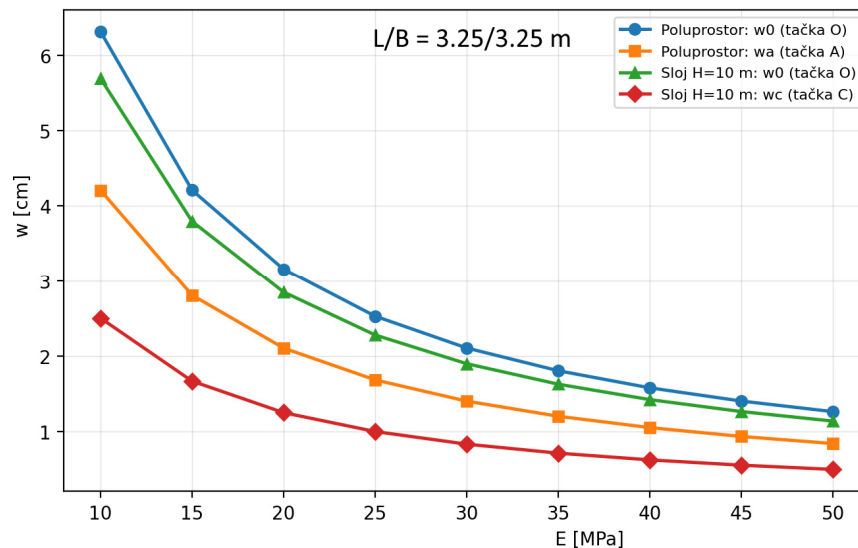


Figure 5: Comparative settlement values for an isolated footing with $L/B = 3.25/3.25$ m for the two analyzed soil models

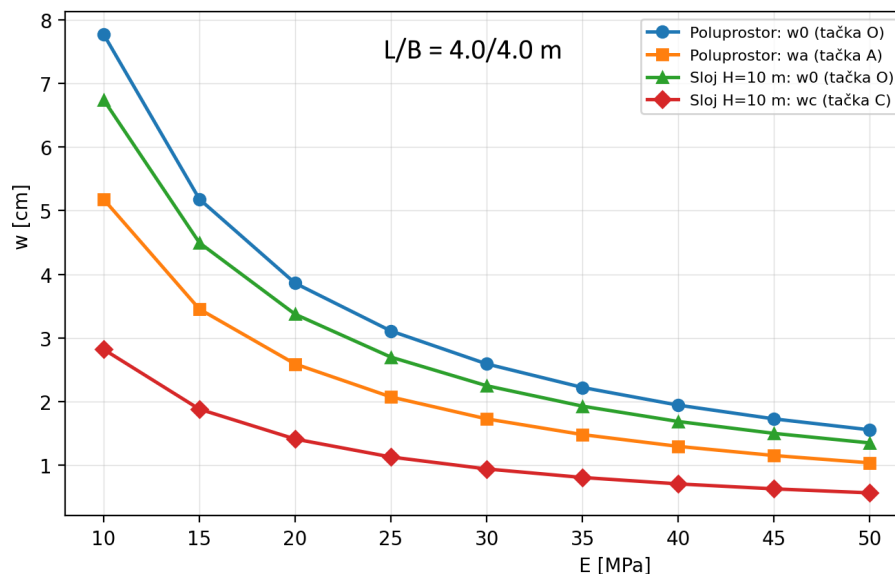


Figure 6: Comparative settlement values for an isolated footing with $L/B = 4.00/4.00$ m for the two analyzed soil models

The diagrams indicate that soil settlement decreases in all analyzed cases with increasing soil deformability (soil stiffness) E , which is consistent with theoretical expectations and the physical behavior of soil. For both soil models, the maximum settlement values occur at the lowest values of E , while with increasing soil stiffness the differences between individual curves gradually decrease. It is also observed that settlements at the characteristic center point (O) are greater than those at points A and C, indicating a more pronounced deformation response of the soil beneath the central part of the footing. The diagrams further show that settlement values at the center point (O) are similar for both soil models, whereas settlement values at the footing edge points, A and C, exhibit significantly larger differences depending on the selected soil model. These observations apply consistently to all three analyzed isolated footing dimensions.

A comparative analysis of the two soil models shows that the elastic half-space model yields higher settlement values than the finite-thickness soil layer model, particularly for lower values of soil stiffness E . This behavior is attributed to the unlimited deformability of the soil with depth in the half-space model, whereas the presence of a rigid base in the finite-thickness model restricts the development of deformations. The differences between the models become more pronounced with increasing footing dimensions, indicating a significant influence of footing geometry on the soil deformation response. These results confirm the importance of selecting an appropriate soil model when analyzing settlements of isolated footings.

4. CONCLUSION

This study analyzed soil stresses and settlements beneath isolated footings for two soil modeling approaches: an elastic half-space of infinite thickness and a finite-thickness soil layer with $H = 10$ m. Settlements were evaluated at characteristic footing points while varying soil deformability (soil stiffness) E in the range of 10–50 MPa at a constant Poisson's ratio of 0.30. The analyses were performed for square isolated footings with plan dimensions of 2.50 m, 3.25 m, and 4.00 m.

It can be concluded that, for both soil models, settlement decreases with increasing soil deformability (soil stiffness). The calculation results indicate that settlements at the footing center point (O) are greater than those at the edge points (A or C). For both soil models and for all analyzed square isolated footing dimensions, settlement values at the center point are approximately the same, whereas this is not the case for the footing edge points. Differences in settlement values at the center point range between 10% and 15%, while differences in settlement at the edge points may reach values of up to 50%, depending on soil deformability.

Finally, it is recommended that, in practical applications of the presented soil models for settlement analysis of isolated footings in building structures, results obtained using both soil models should always be compared. This approach provides increased reliability in structural design and enables verification that settlement values determined by the two soil models remain within acceptable limits.

ACKNOWLEDGEMENTS

This paper is a result of the research conducted within the project grant number 451-03-34/2026-03/200108 supported by the Ministry of Science, Technology and Innovation of the Republic of Serbia, and the CEEPUS project grant "Building Knowledge and Experience Exchange in CFD - RS-1012-10-2425" supported by the Central European Exchange Program for University Studies.

REFERENCES

- [1] M. Djogo, M. Vasić, I. Despotović, and S. Mihajlović, "Geological and Geotechnical Aspects of the Most Significant Deep Landslides in the Danube Area on the Territory of Vojvodina," *Applied Sciences*, Vol. 14(9), p. 3622, <https://doi.org/10.3390/app14093622>, (2024)
- [2] S. Mihajlović, "Projekat fundiranja višespratne zgrade i analiza interakcije temeljne ploče i tla," *Zbornik radova Fakulteta tehničkih nauka u Novom Sadu*, Vol. 35(02), pp. 222–225, <https://doi.org/10.24867/06CG06Mihajlovic>, (2020)
- [3] D. Milović and M. Đogo, "Greške u fundiranju", *Fakultet Tehničkih nauka, Novi Sad (Serbia)*, (2005)
- [4] M. Mohyla, "Experimentally measurement and analysis of stress under foundation slab", *International Journal of GEOMATE*, Vol. 13(35), pp. 128–135, <https://doi.org/10.21660/2017.35.6694>, (2017)
- [5] R. Cajka, J. Labudkova, and P. Mynarcik, "Numerical solution of soil-foundation interaction and comparison of results with experimetal measurements", *International Journal of GEOMATE*, Vol. 11(23), pp. 2116–2122 <https://doi.org/10.21660/2016.23.1208>, (2016)
- [6] W. Pakos and A. Helowicz, "Theoretical and numerical modeling of a shallow foundation stiffness based on the theory of elastic half-space", *Studia Geotechnica et Mechanica*, Vol. 46(4), pp. 302–314, <https://doi.org/10.2478/sgem-2024-0022>, (2024)
- [7] I. F. Collins, "Elastic/plastic models for soils and sands", *International Journal of Mechanical Sciences*, Vol. 47(4–5), pp. 493–508, <https://doi.org/10.1016/j.ijmecsci.2004.12.016>, (2005)
- [8] R. G. Mikola, K. Hatami, and D. Doolin, "Elastic–plastic discontinuous deformation analysis using Mohr–Coulomb model", *Mining Technology*, Vol. 120(3), pp. 148–157, <https://doi.org/10.1179/1743286311Y.0000000006>, (2011)
- [9] J. T. H. Wu and S. C.-Y. Tung, "Determination of Model Parameters for the Hardening Soil Model", *Transportation Infrastructure Geotechnology*, Vol. 7(1), pp. 55–68, <https://doi.org/10.1007/s40515-019-00085-8>, (2020)
- [10] K. Liu, S. L. Chen, and G. Z. Voyiadjis, "Integration of anisotropic modified Cam Clay model in finite element analysis: Formulation, validation, and application", *Computers and Geotechnics*, Vol. 116, p. 103198, <https://doi.org/10.1016/j.compgeo.2019.103198>, (2019)

- [11] J. Jerman and D. Mašin, "Evaluation of hypoplastic model for soft clays by modelling of Nicoll highway case history", *Computers and Geotechnics*, Vol. 134, p. 104053, <https://doi.org/10.1016/j.compgeo.2021.104053>, (2021)
- [12] J. Labudková and R. Čajka, "Comparison of Measured Displacement of the Plate in Interaction with the Subsoil and the Results of 3D Numerical Model", *Advanced Materials Research*, Vol. 1020, pp. 204–209, <https://doi.org/10.4028/www.scientific.net/AMR.1020.204>, (2014)
- [13] Z. Ba, J. Liang, V. W. Lee, and Z. Kang, "Dynamic impedance functions for a rigid strip footing resting on a multi-layered transversely isotropic saturated half-space", *Engineering Analysis with Boundary Elements*, Vol. 86, pp. 31–44, <https://doi.org/10.1016/j.enganabound.2017.10.009>, (2018)
- [14] H. Lemmen, S. Jacobsz, and E. Kearsley, "The influence of foundation stiffness on the behaviour of surface strip foundations on sand", *Journal of the South African Institution of Civil Engineering*, Vol. 59(2), pp. 19–27, <https://doi.org/10.17159/2309-8775/2017/v59n2a3>, (2017)
- [15] Z. Bonić, E. Zlatanović, N. Romić, D. Č. Lukić, and D. Cvetković, "Punching shear capacity of reinforced concrete column footings accounting for the soil–structure interaction effect", *Journal of Building Engineering*, Vol. 46, p. 103706, <https://doi.org/10.1016/j.job.2021.103706>, (2022)
- [16] A. Helowicz, "Analysis of numerical models of an integral bridge resting on an elastic half-space", *Studia Geotechnica et Mechanica*, Vol. 46(4), pp. 337–348, <https://doi.org/10.2478/sgem-2024-0026>, (2024)